

- [16] B. Schiek and K. Schünemann, "Noise of negative resistance oscillators at high modulation frequencies," *IEEE Trans. Microwave Theory Tech.*, vol. MTT-20, pp. 635-641, Oct. 1972.
- [17] A. N. Riddle and R. J. Trew, "A new method of reducing phase noise in GaAs FET oscillators," in *IEEE MTT-S Int. Microwave Symp. Dig.*, 1984, pp. 274-276.

+



Heinz J. Siweris was born in Oberhausen, West Germany, on June 26, 1953. He received the Dipl.-Ing. degree in electrical engineering from the Ruhr-Universität Bochum, West Germany, in 1979.

Since 1979, he has been with the Institut für Hoch- und Höchstfrequenztechnik of the Ruhr-Universität, where he has been working on radiometer systems and low-noise microwave sources.



Burkhard Schiek was born in Elbing, Germany, on October 14, 1938. He received the Dipl.-Ing. and the Dr.-Ing. degrees in electrical engineering, both from the Technische Universität Braunschweig, Germany, in 1964 and 1966, respectively.

From 1964 to 1969, he was an Assistant at the Institut für Hochfrequenztechnik of the Technische Universität Braunschweig, where he worked on frequency multipliers, parametric amplifiers, and varactor phase shifters. From 1969 to 1978, he was involved in MIS interface physics and in the development of MIS varactors. From 1969 to 1978, he was with the Microwave Application Group of the Philips Forschungslaboratorium Hamburg GmbH, Hamburg, Germany, where he was mainly concerned with the stabilization of solid-state oscillators, oscillator noise, microwave integration, and microwave systems. Since 1978, he has been a Professor in the Department of Electrical Engineering, Ruhr-Universität Bochum, Germany, working on high-frequency measurement techniques and industrial applications of microwaves.

## Design Consideration for Frequency-Stabilized MIC IMPATT Oscillators in the 26-GHz Band

NOBUAKI IMAI AND KAZUYUKI YAMAMOTO, MEMBER, IEEE

**Abstract**—A 26-GHz frequency-stabilized MIC IMPATT oscillator using a dielectric resonator has been developed. In designing such an oscillator in the high-frequency range, many parameters affecting frequency stability should be considered. This paper discusses oscillation frequency variations caused by deviations in the resonant frequency of dielectric resonators, in diode reactance, and in the electrical length between the diode and resonator, all of which are due to temperature variation. Design criteria for a highly frequency-stabilized oscillator are also presented. With these techniques, we have obtained an MIC IMPATT oscillator with frequency stability of less than  $\pm 5.0 \times 10^{-5}$ , output power deviation of less than  $\pm 2.0$  dB, and output power of more than 23 dBm over the temperature range of 0°C to 50°C.

### I. INTRODUCTION

RECENTLY, much attention has been focused on microwave integrated circuits (MIC's) for their compactness and low cost. There have been many papers concerning MIC mixers [1], amplifiers [2], oscillators [3]–[5], and transmitter/receiver modules [6].

Frequency-stabilized oscillators are important components for the practical application of MIC's, and many MIC oscillators using dielectric resonators have been devel-

oped in both the microwave frequency range [7]–[11] and higher frequency bands [6], [12].

However, to design frequency-stabilized MIC oscillators in the high-frequency range, more detailed theoretical and experimental investigations are necessary in order to overcome the following problems.

(1) In higher frequency bands, the unloaded  $Q$  factor ( $Q_0$ ) of dielectric resonators decreases, and frequency stabilization becomes difficult.

(2) The resonant frequency of the resonator depends not only on high dielectric constant material, but also on substrate and surrounding materials, especially at high frequencies.

(3) As the oscillation frequency increases, frequency deviation becomes more dependent on variations in the electrical length between the diode and resonator.

(4) To obtain a high-power, highly frequency-stabilized MIC oscillator, circuit parameters ( $Q_0$  and VSWR) need to be optimized.

This paper presents a method to overcome these problems, which facilitates the development of a highly frequency-stabilized MIC oscillator. The first part includes a discussion of resonant frequency deviations in the dielectric resonator due to ambient temperature change, and oscillation frequency variations due to changes in both the

Manuscript received June 7, 1984; revised October 30, 1984.

The authors are with the Radio Transmission Section, Yokosuka Electrical Communication Laboratory, Nippon Telegraph and Telephone Public Corporation, 1-2356 Take, Yokosuka-shi, 238-03 Japan

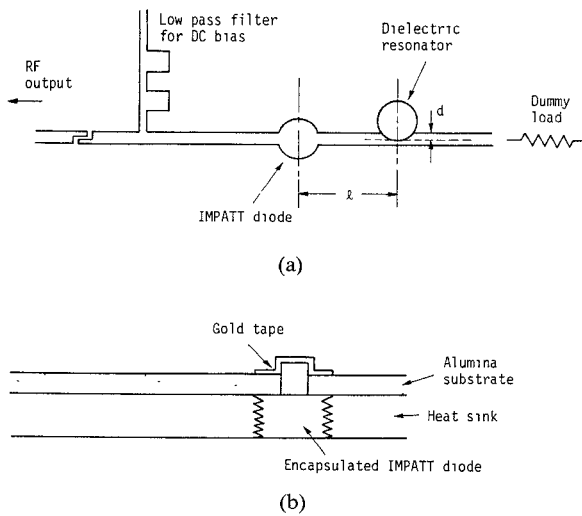


Fig. 1. The construction of a band-reflection-type MIC IMPATT oscillator. (a) Circuit layout. (b) Cross-sectional view.

diode reactance and in the electrical length between the diode and resonator. The paper then proceeds to examine the circuit parameters necessary to obtain a high-power, highly frequency-stabilized oscillator, and discusses the impedance relation between the diode and resonator. On the basis of this research, a 26-GHz high-power, highly frequency-stabilized MIC IMPATT oscillator was achieved.

## II. DESIGN CONSIDERATION FOR FREQUENCY-STABILIZED MIC OSCILLATORS

### A. Oscillator Configuration and Equivalent Circuit

Several types of frequency-stabilized MIC oscillators have been developed [9]–[11]. This paper discusses a band-reflection-type MIC oscillator, as shown in Fig. 1 [9], [13]. A dielectric resonator with a dummy load is coupled to a microstripline behind an IMPATT diode. Output power is delivered from the other part of the microstripline. This type of oscillator is free from spurious oscillation, and the design is simple [13].

The equivalent circuit of this oscillator is shown in Fig. 2. The dielectric resonator, coupled to a microstripline as a band-rejection filter, is represented by a parallel resonant circuit. The impedance, looking into the resonator from the reference plane ( $a - a'$ ), is represented by  $Z_L$ , and that of the diode including the load by  $Z_D$ .

### B. Parameters Affecting Frequency Stability

Oscillation frequency variation is greatly dependent upon deviations in the 1) resonant frequency of the dielectric resonator, 2) diode reactance, and 3) electrical length between the resonator and diode.

The oscillating condition of the oscillator in Fig. 1 is determined by the equation  $Z_D + Z_L = 0$ . It is assumed that the normalized diode reactance  $x_d$  is zero (which could be realized under an appropriate matching condition), and the line length  $l$  is  $l = \frac{1}{4}(2n+2)\lambda_g$  ( $n = 0, 1, 2, \dots$ ). These conditions are optimal in minimizing stabilization loss [13].

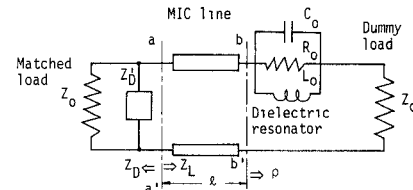


Fig. 2. Equivalent circuit of the oscillator.

Suppose  $x_d$  deviates from 0 to  $\Delta x_d$ , resonant frequency from  $f_{00}$  to  $f_{00} + \Delta f_0$ , and electrical length from  $\theta_0 = \frac{1}{2}(2n+1)\pi$  to  $\theta_0 + \Delta\theta$ . The oscillation frequency deviation ( $\Delta f_T$ ) due to ambient temperature deviation ( $\Delta T$ ) can then be approximated by

$$\begin{aligned} \frac{1}{f_{00}} \cdot \frac{\Delta f_T}{\Delta T} &= \frac{1}{f_{00}} \cdot \frac{\Delta f_0}{\Delta T} - \frac{\rho^2}{2(\rho-1)Q_0} \cdot \frac{\Delta x_d}{\Delta T} - \frac{\rho+1}{2Q_0} \cdot \frac{\Delta\theta}{\Delta T} \\ &= S_1 - S_2 - S_3 \end{aligned} \quad (1)$$

$$S_1 = \frac{1}{f_{00}} \cdot \frac{\Delta f_0}{\Delta T} \quad S_2 = \frac{\rho^2}{2(\rho-1)Q_0} \cdot \frac{\Delta x_d}{\Delta T} \quad S_3 = \frac{\rho+1}{2Q_0} \cdot \frac{\Delta\theta}{\Delta T} \quad (2)$$

where  $Q_0$  is the unloaded  $Q$  factor, and  $\rho$  the VSWR (the resonator was terminated by a matched load at its resonant frequency).  $S_1$ ,  $S_2$ , and  $S_3$  are the temperature coefficients of, respectively, the resonant frequency, the oscillation frequency due to the change in diode reactance, and the oscillation frequency due to the change in electrical length between the diode and resonator.

The temperature coefficient of oscillation frequency

$$\frac{1}{f_{00}} \cdot \frac{\Delta f_T}{T}$$

is directly dependent on  $S_1$ . On the other hand,  $S_2$  and  $S_3$  are inversely proportional to  $Q_0$ . Thus, to decrease the influence of  $S_2$  and  $S_3$  on the temperature coefficient of the oscillation frequency, it is necessary to increase  $Q_0$ .

**1) Resonant Frequency Deviation of the Dielectric Resonator due to Ambient Temperature Change:** In the dielectric resonator of the frequency-stabilized MIC oscillator, the resonant frequency deviation due to ambient temperature change (temperature coefficient of the resonator) should be small and  $Q_0$  large. The latter can be obtained by the radiation-suppressed resonator shown in Fig. 3(b) [14]. In a resonator with this type of structure, the resonant frequency deviation due to ambient temperature depends not only on the temperature coefficient of the high dielectric constant material itself, but also on that of the substrate and the metal cap surrounding the dielectric. In higher frequency bands, the thickness of the substrate  $h_1$  increases relative to the amount of high dielectric constant material.

The resonant frequency of the dielectric resonator in Fig.

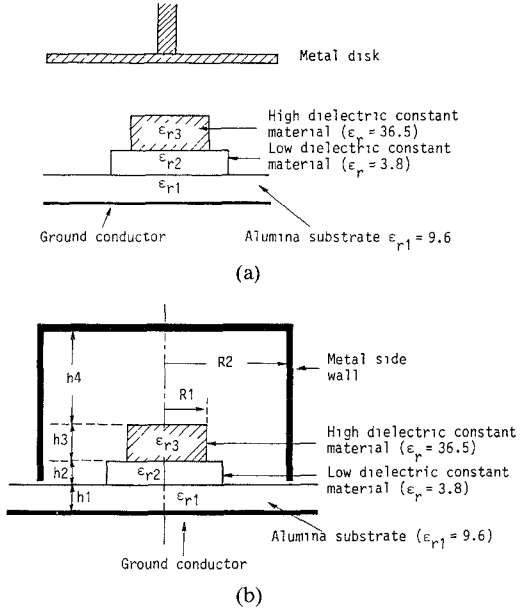


Fig. 3. Construction of dielectric resonators. (a) Conventional dielectric resonator. (b) Radiation-suppressed dielectric resonator.

3(b) can be determined by the following equations [15]:

$$\frac{\xi_3/\xi_4 \tanh \theta_4 \tan \theta_3 - 1}{\xi_3/\xi_4 \tanh \theta_4 + \tan \theta_3} + \frac{p \xi_3/\xi_2 \tan \theta_3 - 1}{p \xi_3/\xi_2 + \tan \theta_3} = 0 \quad (3)$$

$$k_3 \frac{J_0(k_3 R_1)}{J_0'(k_3 R_1)} + k_5 \frac{\frac{K_0(k_5 R_2) I_0(k_5 R_1)}{I_0'(k_5 R_2)} - \frac{K_0'(k_5 R_2) I_0(k_5 R_1)}{I_0'(k_5 R_2)}}{\frac{K_0'(k_5 R_1) - K_0(k_5 R_2) I_0'(k_5 R_1)}{I_0'(k_5 R_1)}} = 0 \quad (4)$$

where

$$p = \frac{\xi_2/\xi_1 \tanh \theta_1 + \tanh \theta_2}{1 + \xi_2/\xi_1 \tanh \theta_1 \tanh \theta_2} \quad (5)$$

$$\theta_i = \xi_i k_i, \quad i = 1, 2, 4 \quad \theta_3 = \frac{\xi_3 h_3}{2} \quad (6)$$

$$k_1 = k_2 = k_3 = k_4 \quad (7)$$

$$k_i^2 = \omega^2 \mu_0 \epsilon_i \pm \xi_i^2, \quad \begin{cases} +i = 1, 2, 4 \\ -i = 3 \end{cases} \quad (8)$$

$$k_5^2 = \xi_5^2 - \omega^2 \mu_0 \epsilon_5 \quad (9)$$

$$\xi_3 = \xi_5 = \delta \pi / h_3 \quad (9)$$

and  $\delta$  denotes a fraction of a half-cycle variation of the field along the resonator length.

A cross section of a radiation-suppressed dielectric resonator is shown in Fig. 4(a). The resonant frequency calculated from the above equations is compared with the experimental resonant frequency ( $f_0 = 26.3$  GHz) shown in Fig. 4(b). They are in good agreement. The resonant frequency is affected very little by increases in  $h_4$ . This demonstrates that the metal cap, used to prevent radiation, has almost no effect on the resonant frequency of the resonator.

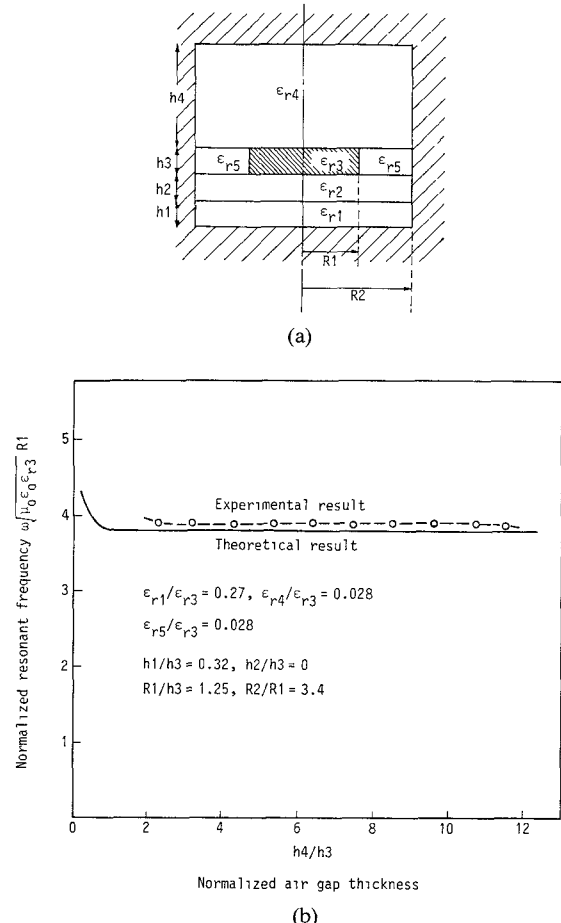


Fig. 4. (a) Cross section of radiation-suppressed dielectric resonator. (b) Resonant frequency of the radiation-suppressed dielectric resonator. The experimental result is for  $\epsilon_{r3} = 36$ ,  $R_1 = 1.2$  mm,  $h_3 = 0.94$  mm. The difference between the experimental and theoretical results is less than 2 percent when the normalized air-gap is between 3 and 9.

The temperature coefficient of the resonator is almost completely determined by that of the high dielectric constant material when this coefficient is high (Fig. 5). However, when it is low, the effect of the substrate becomes significant. When a resonator with a temperature coefficient of less than 10 ppm is necessary, the temperature coefficient of the substrate should be taken into account. The contribution of the metal cap is small even when a metal with a large thermal expansion temperature coefficient such as brass is used.

2) *Frequency Deviation due to the Change in Diode Reactance:* Frequency deviation due to the change in diode reactance ( $S_2$ ) depends on the  $Q_0$  of the dielectric resonator and VSWR  $\rho$ . The calculated  $S_2$ , as a function of  $\rho$  and  $Q_0$ , is shown in Fig. 6. The temperature coefficient of the diode reactance was determined experimentally.  $S_2$  is a minimum at  $\rho = 2$  and increases with increasing  $\rho$ .  $S_2$  is inversely proportional to  $Q_0$ .

On the other hand, the stabilization loss in a band-reflection-type oscillator is expressed by the following equation when the diode reactance is negligible [13]:

$$L(\text{dB}) = -6 + 20 \log \left( 2 - \frac{1}{\rho} \right). \quad (10)$$

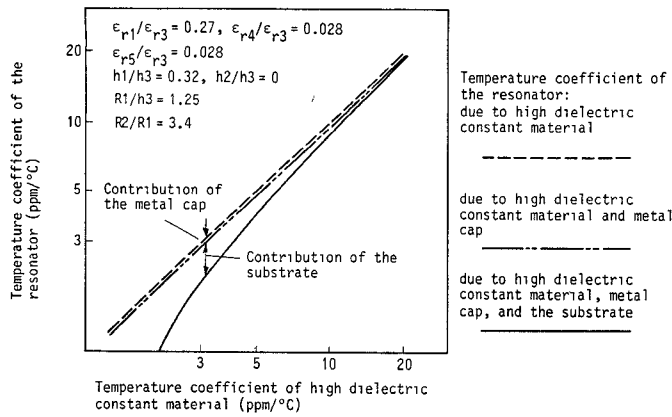


Fig. 5. The calculated dependence of the temperature coefficient of radiation-suppressed dielectric resonator on the temperature coefficient of the high dielectric constant material alone and in the presence of the metal cap and the substrate. The temperature coefficient of thermal expansion for the metal cap (brass) is assumed to be  $\Delta R_2/R_2 = 1.7 \times 10^{-5}/^\circ\text{C}$ , and for the substrate (alumina)  $\Delta R_1/R_1 = 7.9 \times 10^{-6}/^\circ\text{C}$ ,  $\Delta \epsilon_r/\epsilon_r = 110 \times 10^{-6}/^\circ\text{C}$  [16], [17]. The relative dielectric constant and the dimensions of high dielectric constant material are  $\epsilon_r = 36$ ,  $R_1 = 1.2$  mm,  $h_3 = 0.94$  mm, respectively.

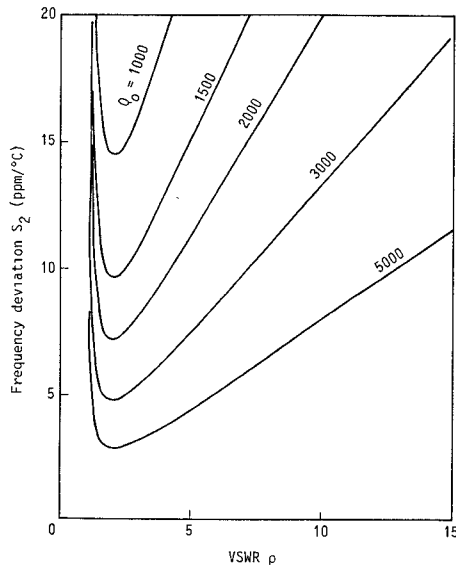


Fig. 6. The dependence of the frequency deviation due to the change in diode reactance by temperature on  $\rho$  and  $Q_0$ .

The loss of output power as a function of  $\rho$ , calculated from (10), is shown in Fig. 7. The loss decreases with increasing  $\rho$ .

To obtain a high-power, highly stabilized oscillator,  $\rho$  should be optimized with respect to both of these aspects. For example, to reduce loss to less than 0.6 dB and obtain a frequency deviation due to a change in the diode reactance with temperature of less than 10 ppm/ $^\circ\text{C}$ , it is necessary to obtain a  $Q_0$  larger than 3000 at a  $\rho$  of 8.

3) *Frequency Deviation due to the Change in Electrical Length between the Diode and Resonator:* For higher frequency bands in the MIC oscillator, the wavelength  $\lambda_g$  becomes short; consequently, the electrical length between the diode and resonator becomes large. The resulting frequency deviation is apparent in the high-frequency range.

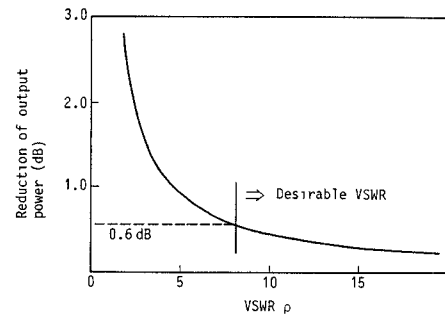


Fig. 7. Reduction of output power versus VSWR when diode reactance is negligible.

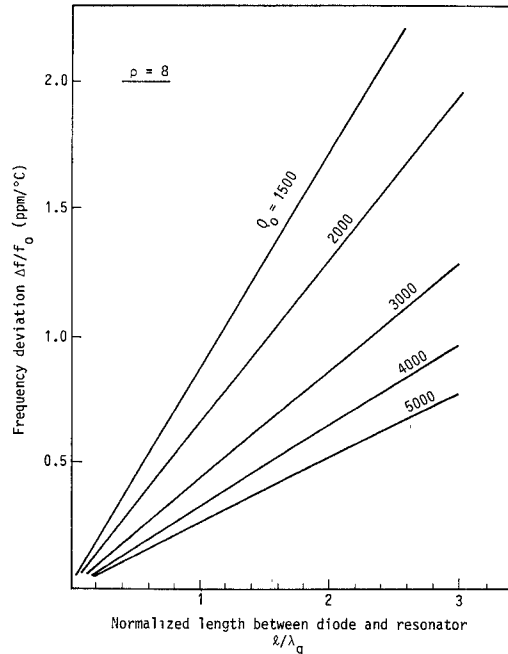


Fig. 8. The frequency deviation due to the change in electrical length between the diode and resonator. Alumina substrate is assumed whose relative dielectric constant  $\epsilon_r$  is 9.6. Characteristic impedance of the line  $Z_0$  is 50  $\Omega$ . Temperature coefficients of thermal expansion are  $\Delta \epsilon_r/\epsilon_r = 110 \times 10^{-6}/^\circ\text{C}$ ,  $\Delta l/l = 7.9 \times 10^{-6}/^\circ\text{C}$ .

If the dielectric constant deviation is  $\Delta \epsilon_r$ , and that of the distance between the diode and resonator is  $\Delta l$ , the frequency deviation can be expressed by the following equation:

$$\frac{\Delta f}{f_0} = -\frac{\rho+1}{Q_0} \cdot \frac{\pi}{\lambda_0} \cdot l \left[ \frac{1}{2} \frac{\Delta \epsilon_{\text{eff}}}{\epsilon_{\text{eff}}} + \sqrt{\epsilon_{\text{eff}}} \frac{\Delta l}{l} \right] \quad (11)$$

where  $\epsilon_{\text{eff}}$  is the effective dielectric constant expressed by

$$\epsilon_{\text{eff}} = \frac{\epsilon_r + 1}{2} + \frac{\epsilon_r - 1}{2} \left( 1 + \frac{10h}{W} \right)^{-1/2} \quad (12)$$

The calculated result of the frequency deviation due to the change in the electrical length between the diode and resonator is shown in Fig. 8. The frequency deviation increases with increasing  $l/\lambda_g$  and decreasing  $Q_0$ . For example, to reduce the frequency deviation  $\Delta f/f_0$  to a negligible value (0.5 ppm) when  $\rho = 8$  and  $Q_0 = 3000$ , the line length should be less than  $1.2 \lambda_g$ .

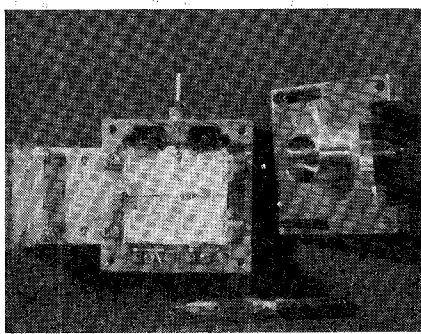
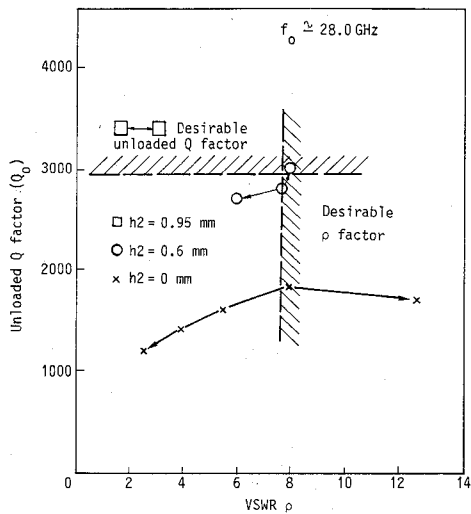


Fig. 9. Photograph of the oscillator.

Fig. 10. Unloaded  $Q$  factor and VSWR of the radiation-suppressed dielectric resonator.  $Q_0$  and  $\rho$  are measured as a function of coupling between stripline and resonator for various values of  $h_2$ .

### III. EXPERIMENT

#### A. Oscillator Configuration

The oscillator configuration used in the experiment is shown in Figs. 1 and 9. An alumina substrate was selected for mechanical strength and a thickness of 0.38 mm was used to avoid spurious modes. A packaged  $S_i$  DDR IMPATT diode was mounted to a ground heat sink with the top electrode connected electrically to the microstrip conductor with gold tape. The dielectric resonator, which is composed of  $\text{Ba}(\text{Zn}_{1/3}\text{Nb}_{2/3})\text{O}_3 - \text{Ba}(\text{Zn}_{1/3}\text{Ta}_{2/3})\text{O}_3$  ceramics, was placed between the diode and the dummy load and bonded to the substrate by aron ceramic adhesive. The distance between the diode and resonator  $l$  was  $l \approx 3/4\lambda_g$ , chosen from the results in Section II-B. The resonant frequency of the radiation-suppressed resonator can be adjusted by a screw that changes the air-gap thickness. The RF power is delivered from the ridged-type waveguide-strip transformer.

#### B. Characteristics of the Dielectric Resonator

The dielectric resonator used for the band-reflection-type oscillator should have a large  $Q_0$  and VSWR. For this purpose, a low dielectric constant material is inserted be-

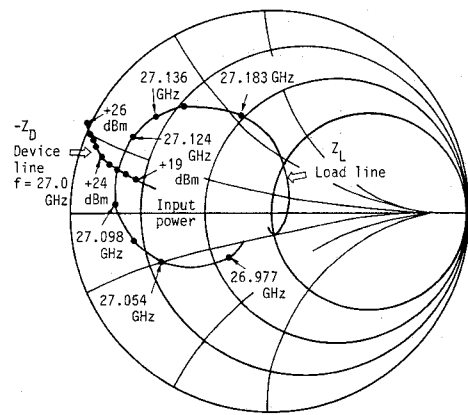
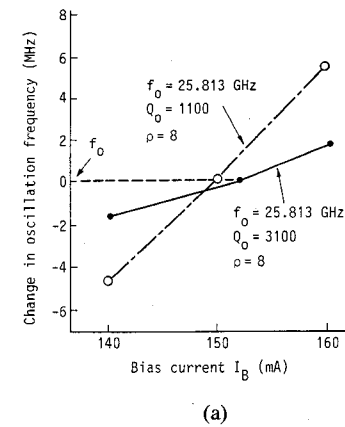
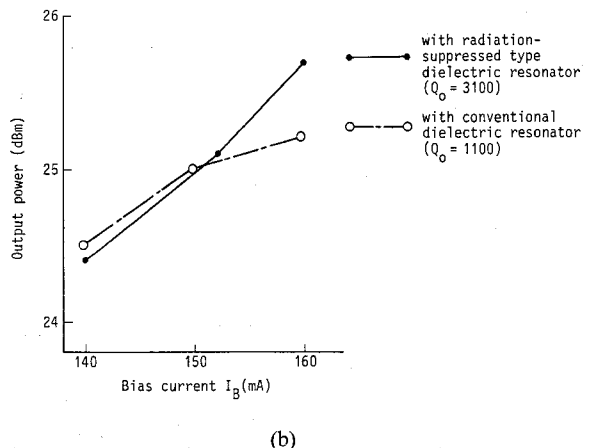


Fig. 11. Relation between the load line and device line for oscillation.



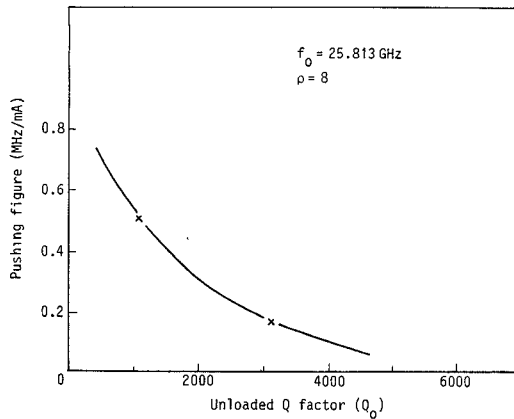
(a)



(b)

Fig. 12. The oscillation frequency and output power versus bias current when  $Q$  factor is varied. (a) Change in oscillation frequency versus bias current. (b) Output power versus bias current.

tween the high dielectric constant material and the substrate. A thickness of  $h_2$ , which provides a high  $Q_0$  and  $\rho$ , was experimentally investigated. Measured  $Q_0$  and  $\rho$  for various  $h_2$  are shown in Fig. 10. The circuit conditions to obtain a high-power and highly frequency-stabilized oscillator ( $\rho > 8$ ,  $Q_0 \geq 3000$ ) are shown in the figure by the shaded area. Considering these conditions,  $h_2 = 0.6$  mm is selected.

Fig. 13. Pushing versus unloaded  $Q$  factor.

### C. Relation between the Load Line and Device Line for Oscillation

To reduce the frequency deviation due to the change in diode reactance by temperature, the load line and device line should intersect at a right angle so that the external  $Q$  factor of the oscillator is large.

The load and device lines, when  $l \approx 3/4\lambda_g$ , are measured and shown in Fig. 11. The matching section around the diode was adjusted so that the diode impedance reactance component is small.

### D. Effect of Increasing Unloaded $Q$ Factor

In a frequency-stabilized MIC oscillator using a dielectric resonator, the frequency deviation due to the change in diode reactance and electrical length decreases with increasing  $Q_0$ , as discussed in Section II. In this section, the effect of increasing  $Q_0$  is experimentally investigated.

The oscillator performances for different  $Q$  factors are measured and shown in Figs. 12 and 13. Frequency stability can be inferred from frequency deviation when the bias current is changed (pushing figure) [18]. The pushing figure, when  $Q_0 = 3100$ , is about half that when  $Q_0 = 1100$ . It is experimentally verified that the frequency deviation due to the change in diode reactance decreases with increasing  $Q_0$ .

### E. Performance of Frequency-Stabilized Oscillator

The oscillator, using a radiation-suppressed high- $Q$  dielectric resonator, was fabricated with the technology discussed above. Experimental results concerning output power and oscillation frequency versus ambient temperature are shown in Fig. 14. The oscillator achieved a frequency variation of less than  $\pm 1.0$  MHz and output power variation of less than  $\pm 2.0$  dB with an output power of more than 23 dBm, over a temperature range of 0°C to 50°C.

No spurious oscillation was observed, and this highly frequency-stabilized MIC oscillator is applicable to high-power local sources.

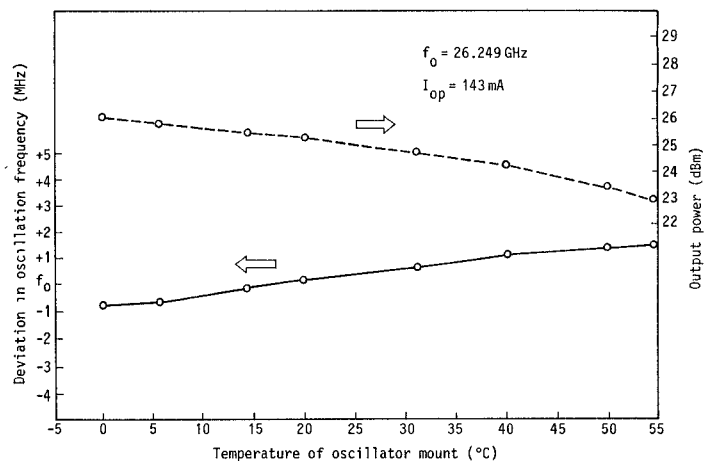


Fig. 14. Temperature dependence of the oscillation frequency and output power.

## IV. CONCLUSION

A 26-GHz frequency-stabilized MIC IMPATT oscillator using a dielectric resonator was developed. Deviations in the resonant frequency of dielectric resonators, in diode reactance, and in the electrical length between the diode and resonator due to temperature variation were investigated. Design criteria for a highly frequency-stabilized oscillator were presented. With these techniques, an IMPATT oscillator with frequency stability of less than  $\pm 5.0 \times 10^{-5}$  and output power deviation of less than  $\pm 22.0$  dB with an output power of more than 23 dBm over the temperature range of 0°C to 50°C was obtained.

## ACKNOWLEDGMENT

The authors wish to thank Dr. K. Kohiyama and Dr. O. Kurita for their encouragement and advice.

## REFERENCES

- [1] H. Ogawa, M. Aikawa, and K. Morita, "K-band integrated double-balanced mixer," *IEEE Trans. Microwave Theory Tech.*, vol. MTT-28, pp. 180-185, Mar. 1980.
- [2] A. Forraye *et al.*, "Design integrated amps with Hi-Lo IMPATT diodes," *Microwaves*, pp. 42-47, Oct. 1976.
- [3] B. S. Glance and M. V. Schneider, "Millimeter wave microstrip oscillator," *IEEE Trans. Microwave Theory Tech.*, vol. MTT-22, pp. 1281-1283, Dec. 1974.
- [4] P. Yen *et al.*, "Millimeter-wave IMPATT microstrip oscillators," in *Proc. 1983 IEEE MTT-S Conf.*, (Boston), pp. 139-141.
- [5] E. J. Denlinger *et al.*, "Microstrip svaractorvaractor-tuned millimeter-wave IMPATT diode oscillators," *IEEE Trans. Microwave Theory Tech.*, vol. MTT-23, pp. 935-958, Dec. 1975.
- [6] E. Hagihara *et al.*, "A 26-GHz miniaturized MIC transmitter/receiver," *IEEE Trans. Microwave Theory Tech.*, vol. MTT-30, pp. 235-242, Mar. 1982.
- [7] J. K. Plourde *et al.*, "A dielectric resonator oscillator with 5 ppm long term stability of 4 GHz," in *1977 IEEE MTT-S Int. Microwave Symp. Dig.*, June 1977, pp. 273-276.
- [8] H. Abe, Y. Takayama, A. Higashisaka, and H. Takamizawa, "A highly stabilized low-noise GaAs FET integrated oscillator with a dielectric resonator in the C band," *IEEE Trans. Microwave Theory Tech.*, vol. MTT-26, pp. 156-162, Mar. 1978.

- [9] G. Satoh, "Stabilized microstrip oscillator using dielectric resonator," in *Proc. 1974 IEEE Int. Solid-State Circuits Conf.*, Feb. 1974, pp. 184-185.
- [10] T. Makino and A. Hashima, "A highly stabilized MIC Gunn oscillator using a dielectric resonator," *IEEE Trans. Microwave Theory Tech.*, vol. MTT-27, pp. 633-638, July 1979.
- [11] S. Shinozaki, T. Hayasaka, and K. Sakamoto, "6-12 GHz transmission type dielectric resonator transistor oscillators," in *1978 IEEE MTT-S Int. Microwave Symp. Dig.*, June 1978, pp. 294-299.
- [12] H. Komizo and Y. Tokumitsu, "Millimeter wave integrated circuits," in *1981 IEEE MTT-S Int. Microwave Symp. Dig.*, June 1981, pp. 179-181.
- [13] K. Kohiyama and K. Momma, "Band reflection type cavity stabilized Gunn oscillator," *Trans. Inst. Electron. Commun. Eng. Japan*, vol. 57-B, no. 2, pp. 98-105, Feb. 1974.
- [14] N. Imai and K. Yamamoto, "A design of high-*Q* dielectric resonators for MIC applications," *Trans. Inst. Electron. Commun. Eng. Japan*, vol. J67-B, no. 5, pp. 497-504, May 1984.
- [15] R. R. Bonetti and A. Atia, "Design of cylindrical dielectric resonators in inhomogeneous media," *IEEE Trans. Microwave Theory Tech.*, vol. MTT-29, pp. 323-326, Apr. 1981.
- [16] W. E. Courtney, "Analysis and evaluation of a method of measuring the complex permittivity and permeability of microwave insulators," *IEEE Trans. Microwave Theory Tech.*, vol. MTT-18, pp. 476-485, Aug. 1970.
- [17] J. E. Aitken, P. H. Ladbrooke, and M. H. N. Potok, "Microwave measurement of the temperature coefficient of permittivity for sapphire and alumina," *IEEE Trans. Microwave Theory Tech.*, vol. MTT-23, pp. 526-529, June 1975.
- [18] T. Makino, "Temperature dependence and stabilization conditions of an MIC Gunn oscillator using a dielectric resonator," *Trans. Inst. Electron. Commun. Eng. Japan*, vol. 62-B, no. 4, pp. 352-358, Apr. 1979.



**Nobuaki Imai** was born in Kochi, Japan, in 1953. He received the B.S. degree in electrical engineering from Nagoya Institute of Technology, Nagoya, Japan, in 1975, and the M.S. degree from Kyoto University, Kyoto, Japan, in 1977.

He joined Yokosuka Electrical Communication Laboratories, Japan, in 1977, and has been engaged in the research of millimeter-wave integrated circuits.

Mr. Imai is a member of the Institute of Electronics and Communication Engineers of Japan.

+



**Kazuyuki Yamamoto** was born in Kyoto, Japan, on July 13, 1946. He received the B.S., M.S., and Ph.D. degrees in electrical engineering, from the University of Kyoto, Japan, in 1969, 1971, and 1982, respectively.

Since joining the Electrical Communication Laboratory, Nippon Telegraph and Telephone Public Corporation (NTT), Tokyo, Japan, in 1971, he has been engaged in the research and development of filters, solid-state circuits, and transmission lines for millimeter and submillimeter wavelength regions. He is currently engaged in the research and development of millimeter-wave integrated circuits for radio communication systems.

Dr. Yamamoto is a member of the Institute of Electronics and Communication Engineers of Japan.

## Boundary Element Method Approach to Magnetostatic Wave Problems

KEN'ICHIRO YASHIRO, MEMBER, IEEE, MORIYASU MIYAZAKI,  
AND SUMIO OHKAWA, SENIOR MEMBER, IEEE

**Abstract** — In this paper, the technique for application of the boundary element method (BEM) to analysis of magnetostatic waves (MSW's) is established. To show the availability of the technique, two types of waveguides for the MSW are studied; one is a waveguide constituting a YIG slab shielded with metal plates and the other is a waveguide consisting of an unshielded YIG slab. With the former structure the results obtained by the present technique are compared with the analytical solutions, and with the latter the BEM is compared with Marcatili's approximate method since there is no analytical solution in this case. Those comparisons are performed successfully for both cases.

The paper concludes that the BEM is useful and effective for analysis of a wide range of MSW problems.

Manuscript received April 9, 1984; revised October 23, 1984.

K. Yashiro and S. Ohkawa are with the Department of Electronic Engineering, Chiba University, 1-33, Yayoi-cho, Chiba, 260 Japan.

M. Miyazaki is with Mitsubishi Electric Corp., Kamakura, Japan.

### I. INTRODUCTION

SEVERAL TYPES OF waveguides for magnetostatic waves (MSW's) have so far been proposed and solved analytically [1]-[3]. Most of them, however, have a simple geometry; as a matter of fact, we may say that an analytical solution can be given only for structures of simple geometry. But from the practical point of view, a numerical solution which can be applied to arbitrary structures is required for an analysis of the MSW problems.

The integral equation formulation has proved to be a powerful tool for obtaining rigorous solutions of electromagnetic and acoustic wave problems. The boundary element method (BEM) [4]-[6] is often used for the calculation of scattering and propagation problems. The BEM is one representative of integral methods and is equivalent to